Study on Planetary Gear Degradation State Recognition Method Based on the Features With Multiple Perspectives and LLTSA

XIHUI CHEN[1,2], HONGYU LI[2], GANG CHENG [ID][2], AND LIPING PENG[1]
[1]College of Mechanical and Electrical Engineering, Hohai University, Changzhou 213022, China
[2]School of Mechatronic Engineering, China University of Mining and Technology, Xuzhou 221116, China

Corresponding author: Gang Cheng (chenxh@cumt.edu.cn)

ABSTRACT Planetary gear is an important part of the transmission system of large electromechanical equipment. Therefore, it is very important to monitor the degradation of the state of the planetary gear. A method for the degradation state recognition of planetary gear based on the features with multiple perspectives and linear local tangent space alignment (LLTSA) algorithm is presented. First, the time domain features of the original vibration signal are extracted, which have the statistical properties and global significance. Then, the detailed features which pay more attention to the detailed information of the vibration signal are extracted on the basis of improved complete ensemble empirical mode decomposition with adaptive noise, and all those features constitute high dimensional original features. In order to solve the problems of information redundancy and interference features, the original features are processed by LLTSA, and the extraction of low dimensional sensitive features can be achieved. Finally, the optimized support vector machine is studied to recognize the low dimensional sensitive features. The result shows that the proposed method can recognize different degradation states of planetary gear accurately and effectively.

INDEX TERMS Degradation state, ICEEMDAN, LLTSA, OSVM, planetary gear.

I. INTRODUCTION

Planetary gear is the important part of the transmission system of large electromechanical equipment, and to ensure the safe and reliable operation of planetary gear, the technologies of condition monitoring and fault diagnosis have received more and more attention [1]–[3]. But in general, planetary gear will undergo a series of degradation processes before fatal fault. The accurate recognition of the current degradation state can effectively prevent further degradation and ultimate failure of planetary gear, and the support for maintenance and management can be provided. Meanwhile, degradation state recognition is also the foundation of planetary gear fault prediction [4], so the study on degradation state recognition of planetary gear is of greater and more practical significance.

Compared with the vibration signal analysis of the fixed-axis gear, it is more difficult to deal with the vibration signal of planetary gear. The main reason is as follows: (1) The planetary gear is a strong nonlinear system composed of multiple components. Its planet gear not only meshes with sun gear, but also engages with inner ring gear, which cause that the vibration excitation is more complicated. (2) The planet gear revolves around its own axis, at the same time, it travels with the planet carrier around the sun gear, and ''the passage effect'' is generated. (3) In general, the installation position of vibration sensor is fixed, and the relative position between the meshing point of planetary gear and the installation position of vibration sensor is always changing. Therefore, in the operation process of planetary gear, the transmission path of the vibration generated by gear meshing to the installation position of vibration sensor is time-varying. These factors cause that the measured vibration signal has more complex characteristics with strong nonlinear, non-stationary and coupling, and the phenomenon of amplitude modulation (AM) and frequency modulation (FM) is more obvious. Therefore, the traditional signal processing methods are not suitable for dealing with the vibration signal of

planetary gear. In addition, although the nature of degradation state recognition is still the problem of pattern recognition, but it is also different from fault diagnosis. Because different degradation states belong to the same type of fault, the differences among the vibration signals are smaller, and the recognition is more difficult. Therefore, the feature extraction is crucial in the degradation state recognition of planetary gear. The traditional feature extraction method for fault diagnosis is to extract the fault feature information from only one perspective. However, when faced with the problem of degradation states recognition, the feature information cannot be extracted fully and completely. Finally, the incomplete feature information will result in a larger recognition error rate. So the feature extraction of planetary gears from different perspectives can enrich the feature information that can reflect the degradation state of planetary gear greatly and effectively, which is advantageous for degradation state recognition of planetary gear.

With respect to feature extraction, the time domain feature contains a wealth of equipment state information, so extracting time domain feature directly from original vibration signal has been widely used. It has statistical properties and global significance and is a useful feature extraction method [5]. In addition, the signal decomposition method is used to convert the original vibration signal into a series of signal components with different varying trends, and then the detailed features are extracted by some nonlinear feature quantization methods. This idea also has been applied to fault diagnosis. Combining these two extraction idea can obtain more full and complete fault features, and the feature extraction from multiple perspectives is more conducive to the degradation state recognition. At present, the signal decomposition and feature analysis methods that can be used for non-stationary signal include short-time Fourier transform (STFT), slow feature analysis (SFA), wavelet transform, empirical mode decomposition (EMD) and so on. SFA is often used in industrial process monitoring, and its improved algorithms, such as global preserving statistics slow feature analysis (GSSFA) and slow feature discriminant analysis (SFDA), have been developed and put forward successively [6]. However, those SFA based methods are generally applied to the monitoring of batch process, and they are more suitable for analyzing the non-stationary signal with slowly varying [7]. But the operation of planetary gear is a continuous process, although the vibration signal of planetary gear has the non-stationary characteristics, but it changes quickly and its frequency is relatively high. So the SFA based methods are not very suitable for processing the vibration signals of planetary gear, and the signal feature with fast varying will be ignored. Wavelet transform and EMD can be applied to the decomposition and processing of the vibration signal of planetary gear. However, wavelet transform does not have the self-adaptability to signal processing, and EMD has serious modal aliasing problem [8]. To solve the modal aliasing problem of EMD, ensemble empirical mode decomposition (EEMD) [9] method was invented. However, the decomposition process of EEMD is not complete, and it will have a larger reconstruction error. Relatively speaking, as an improved form of EMD, the complete ensemble empirical mode decomposition with adaptive noise (CEEMDAN) [10] has a better analytical ability. This method overcomes the problem of mode mixing and has a better reconstruction performance. However, CEEMDAN still has two problems: (1) The obtained intrinsic mode functions (IMFs) include some residual noise; (2) The decomposition result contains ''spurious'' modes. To solve these two problems, the ICEEMDAN was proposed [11]. The vibration signal of planetary gear can be decomposed into a set of high quality IMFs by ICEEMDAN. The features extracted from each IMF pay more attention to the detailed information of vibration signal, which can reflect the detailed differences of different vibration signals. In addition, the single feature extracted from one perspective contains less information and is not comprehensive. Multiple features extracted from each IMF such as permutation entropy, box dimension and energy can enrich the feature information, and they can acquire slight differences among various vibration signals of different degradation states. Based on the above analysis, the original features with multiple perspectives can be constructed using the time domain features and the detailed features extracted from IMFs, and they are advantageous to the degradation state recognition of planetary gear.

With the increasing of original features, information redundancy is also increased. And the correlation between different features will inevitably lead to the existence of interference redundant feature, which interferes with classification and recognition. Therefore, it is also important to reduce the dimension of original features and extract the sensitive features. Currently, there are some dimension reduction methods, such as principal component analysis (PCA) [12] and linear discriminant analysis (LDA) [13], are mainly aimed at linear data. Therefore, these methods are not suitable for processing the vibration signal of planetary gear. In order to deal with the dimension reduction of nonlinear original features, some methods based on kernel function have been proposed by scholars and represented by kernel principal component analysis (KPCA) [14]. However, these methods ignore the useful feature information contained in the high order statistical properties. Additionally, how to determine the kernel function and its parameters is important to the dimension reduction result. Compared with the methods outlined above, the idea of manifold learning is to discover the inherent structure of the low-dimensional smooth manifold, which is embedded in high dimensional nonlinear data space [15]. The difference information from the manifold structure of different states can reflect the characteristics of different states and their evolution process. Therefore, manifold learning can be used to reduce the dimension of original features. The manifold learning method usually includes locality preserving projections (LPP) [16], LLTSA and so on. LLTSA is one of the most widely used and effective methods in manifold learning. It fully considers the topological structure and local information from high dimensional sample features, and the

TABLE 1. The specific definition of each time domain feature.

Features	Definition	Features	Definition
1. Mean square value	$x_{rms} = \sqrt{\dfrac{1}{N}\sum\limits_{i=1}^{N} x_i^2}$	7. Margin index	$L = \dfrac{x_{max}}{x_r}$
2. Absolute Mean value	$|\bar{x}| = \dfrac{1}{N}\sum\limits_{i=1}^{N}|x_i|$	8. Impulsion index	$I = \dfrac{x_{max}}{|\bar{x}|}$
3. Root mean square	$x_r = (\dfrac{1}{N}\sum\limits_{i=1}^{N}(\sqrt{|x_i|}))^2$	9. Waveform index	$W = \dfrac{x_{rms}}{|\bar{x}|}$
4. Variance	$D_x = \dfrac{1}{N-1}\sum\limits_{i=1}^{N}(x_i - \bar{x})^2$	10. Peak index	$C = \dfrac{x_p}{x_{rmx}}$
5. Maximum peak	$x_p = \max|x_i|$	11. Kurtosis index	$K = \dfrac{1}{N}\sum\limits_{i=1}^{N}(\dfrac{x_i - \bar{x}}{\sqrt{D_x}})^4$
6. Peak to peak value	$x_{p-p} = \max(x_i) - \min(x_i)$	12. Skewness index	$S = \dfrac{1}{N}\sum\limits_{i=1}^{N}(\dfrac{x_i - \bar{x}}{\sqrt{D_x}})^3$

dimension reduction result has a smaller information loss rate. The basic idea is to describe the local geometric structure of original features using a low dimensional local tangent space, and then, the dimension reduction of original features is achieved by using a global array of the low dimensional local tangent space [17]. Furthermore, the degradation state recognition of planetary gear can be realized by combining the dimension reduction result and general recognition algorithm.

The remainder of this paper is composed as follows: In section 2, the mathematical model of the proposed method is built. In section 3, the experiment of different degradation states of planetary gear is conducted, and the vibration signals of different degradation states are obtained for the basic of experiment analysis. In section 4, the original features with multiple perspectives consist of two parts, one part is the time domain features, and another part is the detailed features extracted from each IMF. Then, the dimension reduction of original features is achieved by LLTSA, and the low dimensional sensitive features can be obtained. Finally, OSVM is used to recognize different degradation states of planetary gear. In last section, this paper ends with some conclusions.

II. MODEL BUILDING
A. THE HIGH DIMENSIONAL ORIGINAL FEATURES
The original high dimensional features with multiple perspectives consist of two parts, one part is the time domain features of original vibration signal, and they have the statistical properties and global significance in the aspect of feature extraction. Another part is the detailed features extracted from each IMF. The original vibration signal is decomposed into a set of IMFs with strict definition by ICEEMDAN, and the detailed features including permutation entropy, box dimension, energy and absolute mean of AR parameters are extracted from each IMF. The detailed features pay more

attention to the detailed information of vibration signal, which can reflect the local slight differences of various vibration signals.

1) TIME DOMAIN FEATURES OF ORIGINAL VIBRATION SIGNAL
The selected time domain features include 12 parameters, and the specific definition of each time domain feature is shown in Table 1.

2) THE DETAILED FEATURES EXTRACTED FROM IMFS
a: ICEEMDAN
i) EMD
EMD was proposed by Huang, and it can decompose the signal into a series of IMF components with strict definitions [18]. The decomposition process of EMD is as follows:

Step 1: Assuming the original vibration signal is $X(t)$, and its upper and lower envelopes are $u(t)$ and $v(t)$, respectively, Their average envelope is expressed as follows:

$$m(t) = (u(t) + v(t))/2 \qquad (1)$$

Step 2: Subtract $m(t)$ from $X(t)$, and the result is $h_1(t)$.

$$h_1(t) = X(t) - m(t) \qquad (2)$$

$h_1(t)$ insteads of $X(t)$, and the upper and lower envelopes are $u_1(t)$ and $v_1(t)$, respectively. The following process is carried out:

$$\begin{cases} m_1(t) = \{u_1(t) - v_1(t)\}/2 \\ h_2(t) = h_1(t) - m_1(t) \\ \quad\quad \cdots\cdots \\ m_{k-1}(t) = \{u_{k-1}(t) - v_{k-1}(t)\}/2 \\ h_k(t) = h_{k-1}(t) - m_{k-1}(t) \end{cases} \qquad (3)$$

Step 3: The first IMF $d_1(t)$ and the residue $r_1(t)$ can be obtained until $h_k(t)$ meet the strict definitions of IMF.

$$\begin{cases} d_1(t) = h_k(t) \\ r_1(t) = X(t) - h_k(t) \end{cases} \tag{4}$$

Step 4: $r_1(t)$ is regarded as a new signal to repeat the above process until the residue is lower than a certain value. Therefore, the original vibration signal can be expressed as a series of IMFs and a final residue:

$$x(t) = \sum_{k=1}^{K} d_j(t) + r_n(t) \tag{5}$$

However, for the complex non-stationary vibration signal, the IMFs obtained by EMD have the modal aliasing problem.

ii) EEMD
To solve the modal aliasing problem of EMD, EEMD is proposed [9], and its decomposition process of EEMD is expressed as follows:

Step 1: Assuming the original vibration signal is $X(t)$, and generate $X^{(i)}(t) = X(t) + \beta w^{(i)}$, where $w^{(i)}$ is the added white noise with zero mean unit variance, and β is the adjustment coefficient of the added white noise.

Step 2: The vibration signals $X^{(i)}(t), i = 1, 2, \ldots, I$ obtained by adding a total of I times of white noise are decomposed by EMD, respectively. The corresponding IMFs can be obtained, and they are indicated as $d_k^{(i)}$, where $i = 1, 2, \ldots, I, k = 1, 2, \ldots, K$, and it indicates the k-th IMF obtained by EMD for the vibration signal added the i-th white noise.

Step 3: The final IMF $\overline{d_k}$ by EEMD can be obtained by averaging the corresponding $d_k^{(i)}$, and it is expressed as follows:

$$\overline{d_k} = \frac{1}{I} \sum_{i=1}^{I} d_k^{(i)}, \quad k = 1, 2, \ldots, K \tag{6}$$

However, the decomposition process of EEMD is not complete, and the different realizations of vibration signal added white noise may obtain different number of IMFs, making difficult the final averaging.

iii) CEEMDAN
To solve these drawbacks, CEEMDAN is proposed [10], and its decomposition process of CEEMDAN is expressed as follows: Let operator $E_k(\cdot)$ be defined for obtaining the k-th IMF by EMD, and $w^{(i)}$ is the added white noise with zero mean unit variance, then:

Step 1: For the signals $X^{(i)}(t) = X(t) + \beta w^{(i)}$, $i = 1, 2, \ldots, I$, and they are processed by EMD until the first IMF is obtained and calculated, and the first IMF of CEEMDAN is expressed as follows:

$$\tilde{d}_1 = \frac{1}{I} \sum_{i-1}^{I} d_1^{(i)} = \overline{d}_1 \tag{7}$$

Step 2: The first residue can be calculated: $r_1 = X(t) - \overline{d_1}$.

Step 3: Generate the signal $r_1 + \beta_1 E_1(w^{(i)})$, and the second IMF of CEEMDAN is defined and obtained as follows:

$$\tilde{d}_2 = \frac{1}{I} \sum_{i-1}^{I} E_1(r_1 + \beta_1 E_1(w^{(i)})) \tag{8}$$

Step 4: For $k = 2, 3, \ldots, K$, The k-th residue can be calculated: $r_k = r_{k-1} - \tilde{d}_k$.

Step 5: The $(k+1)$-th IMF of CEEMDAN can be obtained on the basis of the above:

$$\tilde{d}_{(k+1)} = \frac{1}{I} \sum_{i-1}^{I} E_1(r_k + \beta_k E_k(w^{(i)})) \tag{9}$$

Step 6: Let $k = k+1$, and repeat Step4-Step6 until the final residue can not be decomposed by EMD. And the original vibration signal can be expressed as follows:

$$\begin{cases} r_K = r_{K-1} - \tilde{d}_K \\ X(t) = \sum_{k=1}^{K} \tilde{d}_j + r_K \end{cases} \tag{10}$$

The decomposition process of CEEMDAN is complete, and the accurate reconstruction of original vibration signal can be realized. The final number of IMFs is determined only by the vibration signal data.

iv) ICEEMDAN
CEEMDAN is an improvement of EEMD, but it still has two shortcomings, and they are stated in the Section 1. Therefore, ICEEMDAN was proposed to overcome those shortcomings, and it is described as follows.

The operator $E_k(\cdot)$ is defined for obtaining the k-th IMF by EMD [19], and the operator $M(\cdot)$ is defined for obtaining the local average envelope of the signal, and it can be noticed that $E1(x) = x - M(x)$. The operator $\langle \cdot \rangle$ is defined for calculating the average value. $w^i(t)$ is the i-th added white noise with zero mean unit variance. $\beta_k = \varepsilon_k std(r_k)$ is used to adjust the signal to noise ratio. For the signal $X(t)$ to be decomposed, the decomposition process of ICEEMDAN is as follows [11].

Step 1: By adding the white noise to the signal $X(t)$, $X(t) + \beta_0 E_1(w^i(t))$ can be obtained. The white noise is added in each time, and EMD process is performed, and the times of the added white noise is I. The average of the corresponding local mean of each EMD result can be calculated. Finally, the first residue can be obtained.

$$r_1 = \left\langle M(X(t) + \beta_0 E_1(w^i(t))) \right\rangle \tag{11}$$

Step 2: Then, the first IMF can be expressed as follows:

$$\tilde{d}_1(t) = X(t) - r_1 \tag{12}$$

Step 3: Further, $r_1(t) + \beta_1 E_1(w^i(t))$ is decomposed by EMD, where $i = 1, 2, \ldots, I$, the average of the local mean of each EMD result is calculated and defined as the second residue; then, the second IMF can be obtained:

$$\tilde{d}_2 = r_1(t) - r_2(t) = r_1(t) - \left\langle M(r_1(t) + \beta_1 E_2(w^i(t))) \right\rangle \tag{13}$$

Step 4: For $k = 3, \cdots, K$, calculate the k-th residue.

$$r_k(t) = \left\langle M(r_{k-1}(t) + \beta_{k-1} E_k(w^i(t))) \right\rangle \quad (14)$$

Step 5: Further, the k-th IMF can be obtained.

$$\tilde{d}_k = r_{k-1}(t) - r_k(t) \quad (15)$$

Step 6: Go to Step 4 for the next k.

Step 7: Through the above process, the original vibration signal of planetary gear can be decomposed into a series of IMFs, and the original vibration signal can be expressed as follows:

$$X(t) = \sum_{k=1}^{K} \tilde{d}_k + r_K(t) \quad (16)$$

where K is the number of the decomposed IMFs, and $r_K(t)$ is the final residue.

ICEEMDAN process reduced the residual noise in the calculation process of each IMF, and the spurious modes are reduced by making use of white noise indirectly [20]. Therefore, ICEEMDAN has more advantages in dealing with the vibration signal with strong nonlinear, non-stationary and coupling.

b: THE DETAILED FEATURES EXTRACTED FROM IMFS

A series of IMFs can be obtained by ICEEMDAN. In order to realize the feature extraction of different degradation states, the first several IMFs, which contain most of the state information, are selected for feature calculation. The feature parameters include permutation entropy, box dimension, energy and absolute mean of auto regression (AR) parameters, they pay more attention to the detailed information of vibration signal, and the local slight differences among various vibration signals of different degradation states can be reflected.

i) PERMUTATION ENTROPY

Permutation entropy is a type of entropy feature proposed by Christoph and Pompe to reflect the stability and complexity of the vibration signal, and it has the advantages of simple, fast calculation, good robustness and so on [21].

Assuming that the discrete vibration signal is $G(i) = \{g(1), g(2), \ldots, g(N)\}$, then the calculation process of permutation entropy can be expressed as follows.

Step 1: The phase space should be first constructed in the calculation process of permutation entropy, the phase space corresponding to the vibration signal $G(i)$ can be constructed as follows:

$$\begin{bmatrix} g(1) & g(1+\tau) & \ldots & g(1+(m-1)\tau) \\ \ldots & \ldots & \ldots & \ldots \\ g(i) & g(i+\tau) & \ldots & g(i+(m-1)\tau) \\ \ldots & \ldots & \ldots & \ldots \\ g(K) & g(K+\tau) & \ldots & g(K+(m-1)\tau) \end{bmatrix}$$
$$(i = 1, 2, \ldots K) \quad (17)$$

where $K = N - (m-1)\tau$, and m and τ are the embedding dimension and delay time, respectively.

Step 2: Each line of Eq. (17) can be regarded as a reconstructed component. Then, the j-th reconstructed component of X will be sorted as shown in Eq. (18):

$$\{g(i+(j_1-1)\tau) \leq g(i+(j_2-1)\tau) \leq \ldots$$
$$\leq g(i+(j_m-1)\tau)\} \quad (18)$$

where $j_1, j_2, \ldots, j_m$ are the indexes of each element of the reconstructed component. If two or more elements in the reconstructed component are equal, they are arranged in the order of original time.

Step 3: A series of symbol sequences can be obtained for an arbitrary vector in m dimensional space:

$$S(l) = (j_1, j_2, \ldots, j_m) \quad l = 1, 2, \ldots, k \quad (19)$$

Step 4: For the symbol sequence $S(l)$ obtained from Eq. (19), the number of occurrences in all symbol sequences can be expressed as f, and the occurrence frequency of each symbol sequence can be expressed as follows:

$$P_i = \frac{f}{N - (m-1)\tau} \quad (20)$$

The permutation entropy of different symbol sequences of the original vibration signal $G(i)$ can be calculated as follows:

$$E_p(m) = -\sum_{i=1}^{m} P_i \ln P_i \quad (21)$$

Step 5: Furthermore, the permutation entropy is normalized:

$$E_p(m) = \frac{E_p(m)}{\ln(m!)} \quad (22)$$

where $0 \leq E_p \leq 1$, and the value of E_p reflects the stability and complexity of the vibration signal $G(i)$.

ii) BOX DIMENSION

The fractal dimension is widely used in the extraction and quantification of fault feature, and the box dimension is a typical fractal dimension. It can reflect the dynamic changes of the signal generated by the mechanical system [22].

Suppose that the discrete vibration signal is $G(i) \subset Y$, and Y is a closed set on R^n. Then, the calculative process of box dimension can be expressed as follows.

Step 1: R^n is divided by ε, which is a very fine grid. $N(\varepsilon)$ is the minimum number of grids when Y is fully covered.

Step 2: Gradually enlarge the grid until the scale of the grid is $k\varepsilon$, then

$$a = \max\{G_{k(i-1)+1}, G_{k(i-1)+2}, \ldots, G_{k(i-1)+k+1}\}$$
$$b = \min\{G_{k(i-1)+1}, G_{k(i-1)+2}, \ldots, G_{k(i-1)+k+1}\}$$
$$P(k\varepsilon) = \sum_{i=1}^{N/k} |a - b| \quad (23)$$

where $i = 1, 2, \ldots, N/k$, $M < N$, $k = 1, 2, \ldots, M$, and N is the length of the signal.

Step 3: The grid count can be calculated according to the following formula:

$$N(k\varepsilon) = P(k\varepsilon)/k\varepsilon + 1 \tag{24}$$

where $N(k\varepsilon) > 1$.

Step 4: A good linear scale-free zone in the graph of $\lg k\varepsilon - \lg N(k\varepsilon)$ is then calculated, and the starting point k_1 and the termination point k_2 are set. Then,

$$\lg N(k\varepsilon) = a \lg k\varepsilon + b k_1 \leq k \leq k_2 \tag{25}$$

Step 5: Finally, the slope of the straight line can be calculated using the least square method.

$$\hat{a} = -\frac{(k_2 - k_1 + 1)\sum \lg k \lg N(k\varepsilon) - \sum \lg k \sum \lg N(k\varepsilon)}{(k_2 - k_1 + 1)\sum \lg^2 k - (\sum \lg k)^2} \tag{26}$$

Then, the box dimension D_B of $G(i)$ can be calculated.

$$D_B = \hat{a} \tag{27}$$

iii) ENERGY

The energy of vibration signal can reflect the difference in its vibration intensity. More importantly, when the original signal is decomposed, the energy information can be highlighted in different components, which is useful for extracting feature information of different degradation states. For the various IMFs obtained by ICEEMDAN, the energy contained in each IMF is important for the processing of non-stationary and time-varying signals.

For the discrete vibration signal $G(i) = \{g(1), g(2), \ldots, g(N)\}$, the calculation formula of energy is expressed as follows:

$$E = \sum_{i=1}^{N} g(i)^2 \tag{28}$$

iv) ABSOLUTE MEAN OF AR PARAMETERS

AR model is a type of time series analysis method, and the model parameters have important connection with the important information about the system state [23]. Therefore, the AR model parameters can also be used for feature extraction.

Suppose that the discrete vibration signal $G(i) = \{g(1), g(2), \ldots, g(N)\}$, and its AR model can be established as follows:

$$G(i) = \sum_{k=1}^{n} \varphi_k G(i-k) + e(i) \tag{29}$$

where $\varphi_k (k = 1, 2, \ldots, n)$ is the model parameter, n is the order number, and $e(i)$ is the model residual. φ_k can express the inherent characteristics of vibration system, which can be solved by using the Burg algorithm [24]. Considering to the state information of the signal is mainly determined by the first several model parameters, the AR model are constructed for the selected IMFs, and the absolute mean value of the first several model parameters is taken as the feature value of the corresponding IMF.

B. LLTSA

LLTSA is one of the primary methods to reduce the dimension of nonlinear feature data. The core idea is to represent the local geometric properties of these points using the neighborhood tangent space formed by the sample points and their nearest neighbors. Then, the local low dimension coordinates are determined by the projection of the sample points on the tangent space. Finally, the global low dimensional coordinates are obtained using the obtained local low dimension coordinates, and the dimension reduction of original features can be achieved [25]. Suppose there is a feature set X that is constituted by m samples as follows:

$$X = \begin{bmatrix} x_{11} & x_{12} & \ldots & x_{1n} \\ x_{21} & x_{22} & \ldots & x_{2n} \\ \ldots & \ldots & \ldots & \ldots \\ x_{m1} & x_{m2} & \ldots & x_{mn} \end{bmatrix} \tag{30}$$

Then, LLTSA is used to process X, and the low dimensional feature set Y can be obtained.

$$Y = \begin{bmatrix} y_{11} & y_{12} & \ldots & y_{1d} \\ y_{21} & y_{22} & \ldots & y_{2d} \\ \ldots & \ldots & \ldots & \ldots \\ y_{m1} & y_{m2} & \ldots & y_{md} \end{bmatrix} \tag{31}$$

where $Y \subseteq R^d (d << n)$.

The specific process of LLTSA is as follows.

Step 1: The local neighborhood of the sample point x_i $(i = 1, 2, \ldots, m)$ is constructed based on the neighborhood parameter k.

$$X_i = [x_i^{(1)}, x_i^{(2)}, \ldots, x_i^{(k)}] \tag{32}$$

Step 2: The local coordinate of the neighborhood is determined.

$$\Phi = [\theta_i^{(1)}, \theta_i^{(2)}, \ldots, \theta_i^{(k)}] \tag{33}$$

where $\theta_i^{(j)} = Q_i^T (x_i^{(j)} - \bar{x}_i)$ $(j = 1, 2, \ldots, k)$, Q_i is an orthogonal basis in the neighborhood, and $\bar{x}_i$ is the mean of the neighborhood of x_i.

Step 3: The global arrangement of all local coordinates is performed, which the key is to ensure that the reconstruction error of the global alignment is minimized, and it can be expressed as follows:

$$\min_{L_i, Y_i} = \sum_i \|E_i\|^2 = \min_{L_i, Y_i} \sum_i \left\| Y_i(I - ee^T/k) - L_i\Phi_i \right\|^2 \tag{34}$$

where Y_i is the global representation of the local tangent space coordinate for the first i sample points, and L_i is the mapping matrix. Then, after mathematical deduction, the above formula can be converted into the following form:

$$\min_Y \|YSW\| = \min_Y tr(YSWW^T S^T Y^T) \tag{35}$$

where $S = [S_1, S_2, \ldots, S_m]$ is the selection matrix, and $Y_i = S_i Y$, $W = diag(W_1, W_2, \ldots, W_m)$, where W_i can be calculated as follows:

$$W_i = (I - ee^T/k)(I - \Phi_i^+ \Phi_i) \tag{36}$$

By adding a constraint $Y^T Y = I$, we can make sure that Eq. (35) has a unique solution. Then, the eigenvectors corresponding to the non-null eigenvalues of the first d can form a feature matrix, and it is the global coordinate mapping that is corresponding to the low dimensional nonlinear manifold of the original features set X.

III. EXPERIMENT OF DIFFERENT DEGRADATION STATES OF PLANETARY GEAR

The experiment of different degradation states of planetary gear was conducted in the mechanical fault simulation bench. The experimental system is shown in Fig.1, and it includes a planetary gearbox with two stages, a controllable motor, a fixed-axis gearbox, a brake system and a data acquisition system. The basic parameters of planetary gearbox with two stages are shown in Table 2. The vibration signals of different degradation states can be measured by using acceleration sensors, and the specific installation of acceleration sensors is shown in Fig. 2. The normal state of sun gear and four degradation states of a tooth root crack are simulated, and they are normal, 25% crack, 50% crack, 75% crack and 100% crack. The various gear states are shown in Fig. 3. During the duration of the experiment, the motor output frequency is set to 45 Hz, and the load is set to 13.5 Nm. Meanwhile, the sampling frequency is set to 13017 Hz. Each degradation state collects 50 groups of samples, and each sample includes 5120 data points.
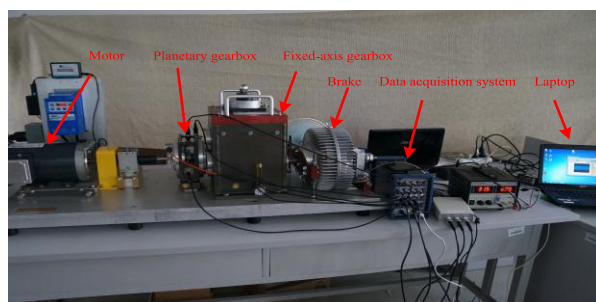

FIGURE 1. Experiment of degradation states for planetary gear.

TABLE 2. Basic parameters of planetary gearbox with two stages.

	The first stage planetary gear			The second stage planet gear		
	Sun gear	Planet gear	Ring gear	Sun gear	Planet gear	Ring gear
Teeth	20	40	100	28	36	100

IV. EXPERIMENTAL ANALYSIS AND DATA PROCESSING

The analytical flowchart of the proposed method is shown in Fig. 4. The various degradation states of planetary gear are simulated, and the obtained vibration signals are shown in Fig. 5.

It can be found from Fig. 5 that there is a certain difference in the vibration signals of different degradation states of planetary gear. The vibration signal of normal state is relatively
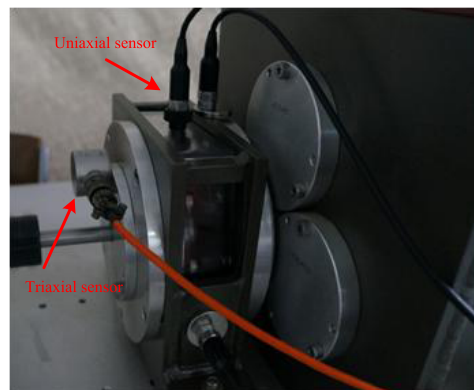

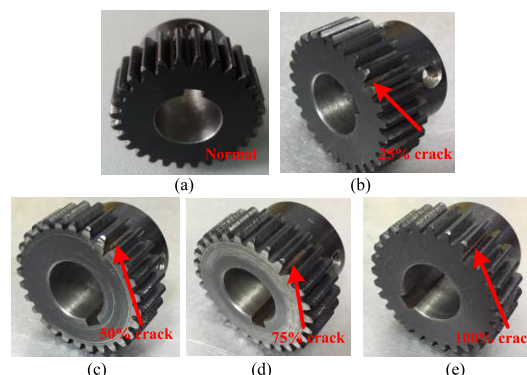FIGURE 2. Specific installation of acceleration sensors.

FIGURE 3. Various degradation states of planetary gears: (a) normal. (b) 25% crack, (c) 50% crack, (d) 75% crack, (e) 100% crack.
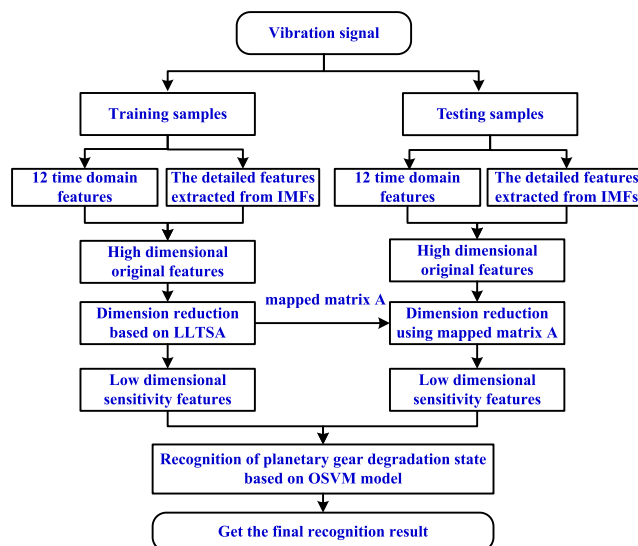

FIGURE 4. Experimental analytical flowchart.

stable, and there is no significant impact, and the vibration signal of 25% crack has obvious impacts. However, the planetary gear states cannot be determined only by analyzing vibration signal in time domain. Therefore, the vibration signals require further processing.

According to the proposed method, the original features with multiple perspectives are extracted. Firstly, 12 time
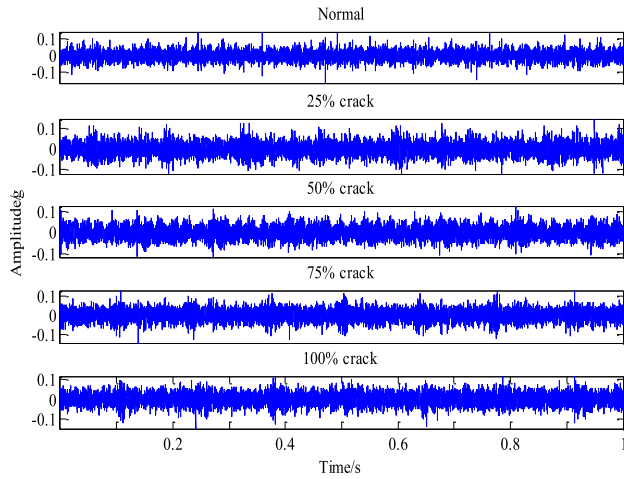
FIGURE 5. The vibration signals of various degradation states.

domain features of original vibration signals are extracted. In order to compare the sensitivity of time domain features to degradation states, 20 groups of samples of each state are selected and analyzed, and they are shown in Fig. 6.
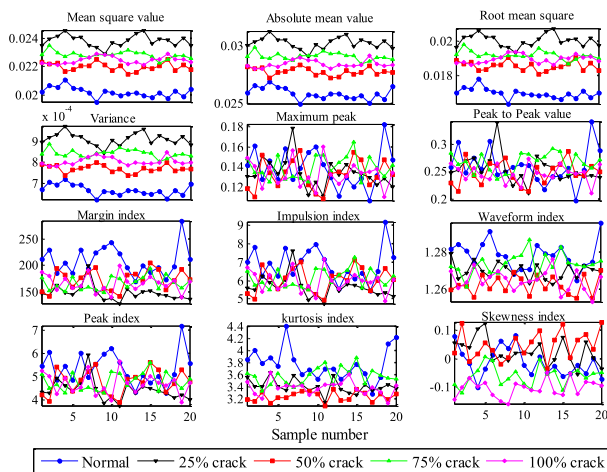

FIGURE 6. The calculation results of time domain features.

It can be found from Fig. 6 that the first four features can be roughly distinguished between the normal and various crack states. However, the features of 50% crack, 75% crack and 100% crack are partially overlapped. The rest of the time domain features, compared with the first four features, show a more chaotic phenomenon. These features can still distinguish individual state, but the effect is not ideal. Therefore, although the time domain features contain a great deal of state information, but they are not enough to accurately judge the various degradation states.

Next, the detailed features extraction is conducted. The key of the detailed features extracted from IMFs is ICEEMDAN. To show that the decomposition effect of ICEEMDAN is better than that of CEEMDAN and EEMD, the vibration signal of 75% crack is decomposed by using these three methods as

an example. There are two important parameters that must be defined. One parameter is the amplitude of the added white noise, and in this paper, it is set to $0.2std$, and std is the standard deviation of vibration signal. Another parameter is the overall average number, and it is set to 100. The decomposition results are shown in Fig. 7, Fig. 8 and Fig. 9, respectively.
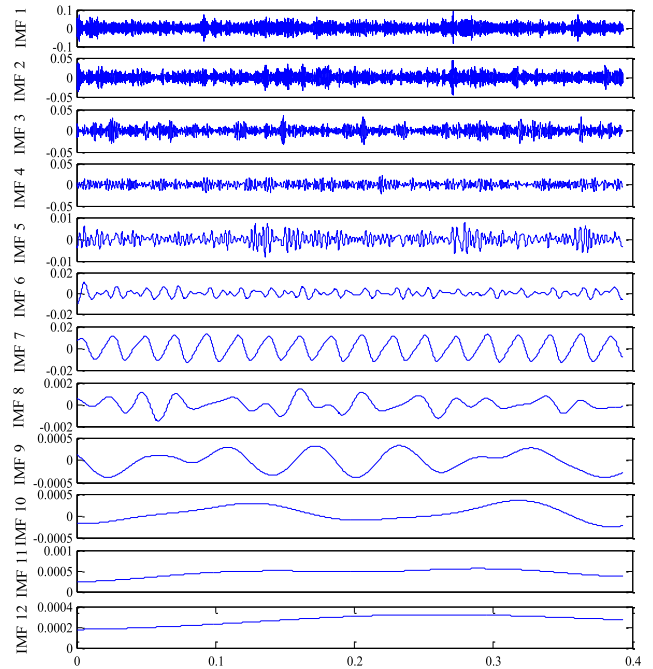
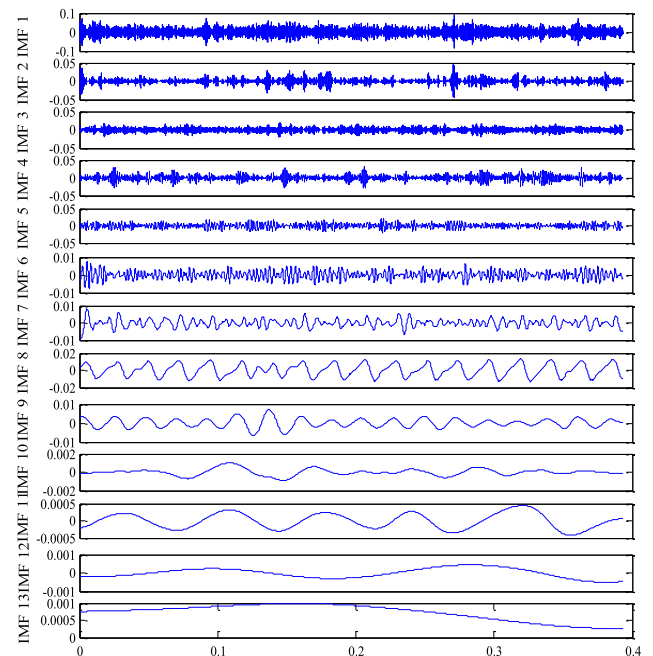

FIGURE 7. The decomposition result of EEMD.

FIGURE 8. The decomposition result of CEEMDAN.

By comparison, it can be found that there is a phenomenon of modal aliasing in the decomposition result of EEMD,
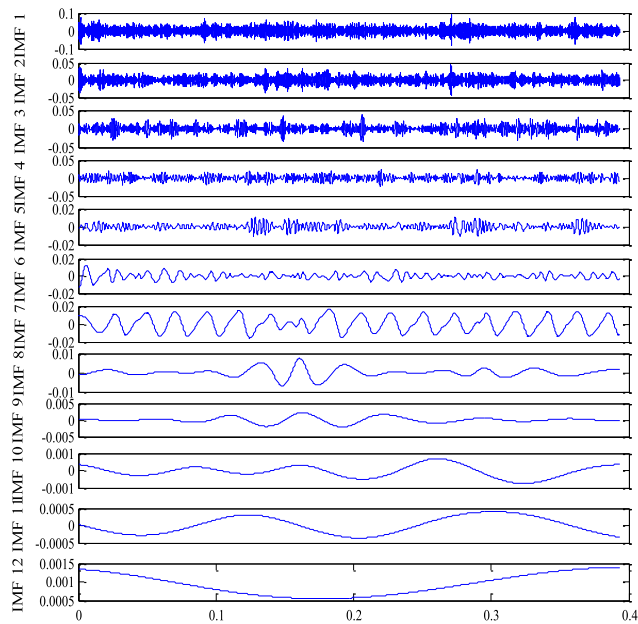
FIGURE 9. The decomposition result of ICEEMDAN.

such as IMF8 and IMF9 in Fig. 7. The actual physical meanings of IMFs become unclear with the appearance of modal aliasing phenomenon, and furthermore, the extracted features will be inaccurate. Meanwhile, there is an obvious spurious mode (IMF3) in the decomposition result of CEEMDAN. The appearance of spurious components will lead to the extraction of useless features, and will increase the difficulties in the subsequent analysis. However, there are no such problems in the result of ICEEMDAN. Therefore, through the comparison and analysis of the above results, ICEEMDAN has a better decomposition effect.

The first nine IMFs contain almost 95% of the total energy of original vibration signal. Therefore, for the first nine IMFs obtained by ICEEMDAN, permutation entropy, box dimension, energy coefficient and the absolute mean of the first five AR parameters of each IMF are calculated. There are two parameters that are required to be set in the calculating process of permutation entropy: embedding dimension m and time delay τ. In general, the range of embedding dimension should be 3-7. When m is too small, the algorithm will lose effectiveness and actual meaning. In contrast, the calculation time will increase, and more importantly, the algorithm will not be able to effectively respond to subtle changes. The delay time has little effect on the calculation result. Therefore, in this paper, m is set to 6 and τ is set to 3. To illustrate the effectiveness of the selected features, the detailed features extracted from IMFs for each state are shown in Fig. 10.

Because different degradation states of planetary gear still belong to the same fault type, so their original vibration signals are very similar. For Fig. 10, to analyze the detailed features extracted from IMFs obtained by ICEEMDAN, it can be found that there are relatively significant differences
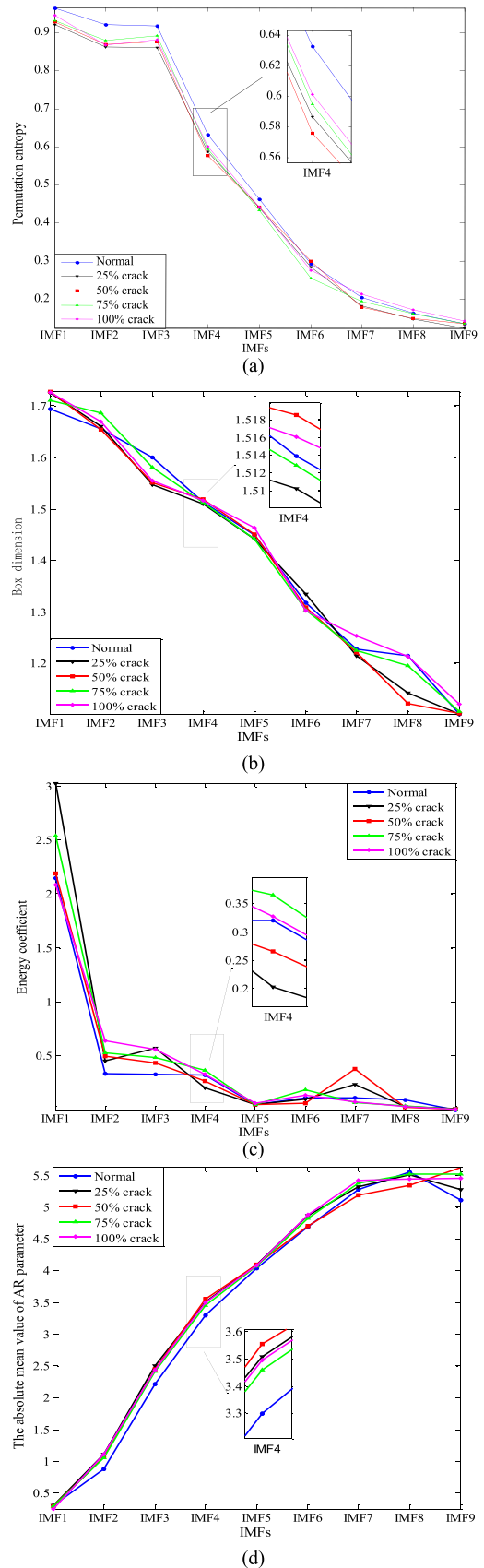

FIGURE 10. The detailed features extracted from IMFs. (a) Permutation entropy. (b) Box dimension. (c) Energy coefficient. (d) The absolute mean of the AR parameter.

TABLE 3. The recognition results of various degradation states of planetary gear.

Method	Normal	25% crack	50% crack	75% crack	100% crack	Average recognition rate
LLTSA	93.33%	100%	100%	100%	100%	98.67%
PCA	100%	63.33%	96.67%	56.67%	40%	71.33%
KPCA	76.67%	90%	76.67%	86.67%	70%	80%
LPP	100%	93.33%	100%	90%	96.67%	96%
NPE	86.67%	100%	83.33%	96.67%	93.33%	92%

between the detailed features of some IMFs among different degradation states, such as the permutation entropy of IMF3, the box dimension of IMF8, the energy coefficient of IMF1, the absolute mean of the AR parameter of IMF9 and so on. In addition, it also can be found that the detailed features of different degradation states of planetary gear are very similar in some IMFs, which are not easy to be distinguished from rough analysis. However, after amplification, the detailed features of different degradation states still have a slightly difference. Combining the above detailed features can reflect the operation status of planetary gear from different perspectives, so as to enrich the feature information that can reflect the degradation state of planetary gear greatly and effectively.

Based on the feature extraction process outlined above, original features with 48 dimensions are established. However, the increasing of feature dimension would result in information redundancy. Although the features with small differences can provide some differentiated information, but they still have invalid features. And the correlation between different features will inevitably lead to the existence of interference redundant information, which interferes with classification and recognition. So the dimension reduction should be conducted, and the sensitive features which can best reflect the degradation states of planetary gear can be obtained from original features, and LLTSA algorithm is used in this paper. Prior to this, two LLTSA parameters are required to be defined: the target dimension d and the neighbor parameter k. In this paper, d is set to 3 and k is set to 8. Then, the dimension of the training samples is reduced by LLTSA, and the mapping matrix can be obtained. Finally, the dimension reduction of test samples is carried out according to the mapping matrix obtained from the training samples. The dimension reduction result of all samples by LLTSA is shown in Fig. 11(a). Meanwhile, In order to illustrate the effectiveness of LLTSA, other dimension reduction methods: PCA, KPCA, LPP and neighborhood preserving embedding (NPE) are used to perform comparative analysis. The dimension reduction results of all samples by PCA, KPCA, LPP and NPE are shown in Fig. 11(b)-Fig. 11(e).

It can be found from the comparison among Fig. 11(a)-Fig. 11(e) that the sensitive features obtained by PCA can distinguish the states of normal and 50% crack.

However, the sensitive features of 25% crack, 75% crack and 100% crack have a serious aliasing phenomenon, and it is difficult to separate those three states. In the dimension reduction result of KPCA, due to the introduction of kernel function, the separability of sensitive features among various degradation states has improvement compared with the dimension reduction result by PCA. It can be found that the states of 25% crack and 75% crack can be roughly separated. But the states of normal, 50% crack and 100% crack are still hard to distinguish completely. In the dimension reduction results by LPP and NPE, the separability of sensitive features among various degradation states of planetary gear has further improvement. But there are still some slight overlapping among them, such as the states of 25% crack and 75% crack in the dimension reduction result by LPP, the states of normal and 50% crack in the dimension reduction result by NPE. After the treatment by above methods, it can be seen that the clustering effect of the sensitive features of different degradation states is not ideal. On the contrary, in the dimension reduction result by LLTSA, each degradation state of planetary gear has been well differentiated. It can be proved that LLTSA can get better result than those dimension reduction methods for the original features.

To quantitatively describe the dimension reduction result by LLTSA, the recognition rate of each planetary gear state is calculated in the following. Support vector machine (SVM) is a machine learning method developed in the framework of statistical learning theory, and it is widely used in pattern recognition [26], [27]. However, the SVM parameters, which are the penalty factor C and the kernel function parameter σ, have a significant influence on the recognition result. Taking into account the genetic algorithm can be used to achieve the optimization of complex systems [28], so it is applied to the parameters optimization of SVM. And OSVM is used to classify and recognize the sensitive features. Firstly, based on the samples obtained in the experiment, 20 groups of samples of each planetary gear state are used for training, and 30 groups of samples are used for testing. Then, the optimal parameters of SVM are found by genetic algorithm as follows: $C = 16.0244$, $\sigma = 4.7739$. Finally, the recognition result based on optimal parameters is shown in Table 3. In the same way, for the sensitive features obtained by PCA,
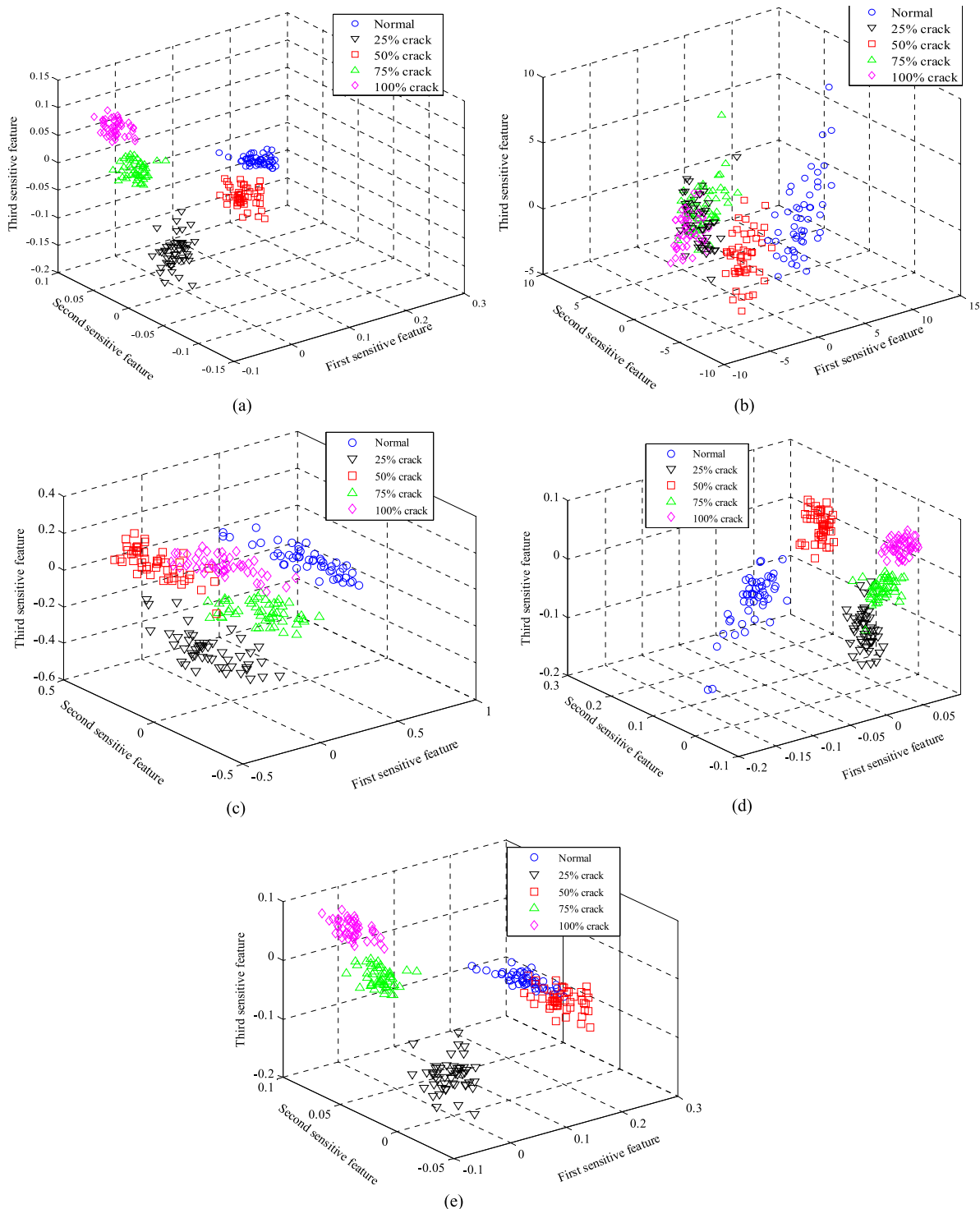
FIGURE 11. The dimension reduction results by LLTSA, PCA, KPCA, LPP and NPE. (a) The dimension reduction result by LLTSA. (b) The dimension reduction result by PCA. (c) The dimension reduction result by KPCA. (d) The dimension reduction result by LPP. (e) The dimension reduction result by NPE.

KPCA, LPP and NPE, each method can also obtain the corresponding optimal parameters of OSVM respectively. OSVM is also used to recognize the sensitive features obtained by PCA, KPCA, LPP and NPE, respectively, and the recognition results of various degradation states of planetary gear are also shown in Table 3.

Table 3 shows that the average recognition rate of different degradation states based on LLTSA is 98.67%, and there are only two recognition errors in normal state. The average recognition rates of different degradation states based on PCA, KPCA, LPP and NPE are 71.33%, 80%, 96% and 92%, respectively. Their recognition results are worse than that

processed by LLTSA. Therefore, it can be further proved that LLTSA has the advantages in the dimension reduction of the original features with non-stationary and nonlinear. And the proposed method of degradation state recognition of planetary gear based on the features with multiple perspectives and LLTSA is effective.

V. CONCLUSIONS

A method for the degradation state recognition of planetary gear based on the features with multiple perspectives and LLTSA is presented. The original features with multiple perspectives consist of two parts, one part is the time domain features of original vibration signal. Another part is the detailed features, and they include permutation entropy, box dimension, energy coefficient and the absolute mean of the first five AR parameters of each IMF which is obtained by ICEEMDAN. Meanwhile, the experiment shows that ICEEMDAN can achieve a better result than EEMD and CEEMDAN in adaptive signal decomposition. In this manner, the constructed original features have the problems of information redundancy and excessive dimension, so LLTSA is used for dimension reduction. And in order to illustrate the effectiveness of LLTSA, the processing result of LLSTA is compared with that of PCA, KPCA, LPP and NPE. The result shows that LLTSA has better dimension reduction ability compared with PCA, KPCA, LPP and NPE, and the samples with different degradation states can be separated effectively. Finally, OSVM is used to classify and recognize the low dimensional sensitive features obtained by different dimension reduction methods. And it can be found that the average recognition rate of different degradation states processed by LLTSA reaches 98.67%, and it is superior to the recognition rates of different degradation states processed by other methods. Therefore, it can be proved that the proposed method of degradation state recognition of planetary gear based on the features with multiple perspectives and LLTSA is effective.

REFERENCES

[1] X. Chen, G. Cheng, Y. Li, and L. Peng, "Fault diagnosis of planetary gear based on entropy feature fusion of DTCWT and OKFDA," *J. Vib. Control*, vol. 24, no. 21, pp. 5044–5061, 2018.

[2] X. Chen and Z. Feng, "Time-frequency analysis of torsional vibration signals in resonance region for planetary gearbox fault diagnosis under variable speed conditions," *IEEE Access*, vol. 5, pp. 21918–21926, 2017.

[3] Z. Qiao, Y. Lei, J. Lin, and F. Jia, "An adaptive unsaturated bistable stochastic resonance method and its application in mechanical fault diagnosis," *Mech. Syst. Signal Process.*, vol. 84, pp. 731–746, Feb. 2017.

[4] X. Zhao, M. J. Zuo, Z. Liu, and M. R. Hoseini, "Diagnosis of artificially created surface damage levels of planet gear teeth using ordinal ranking," *Measurement*, vol. 46, no. 1, pp. 132–144, 2012.

[5] S. Huang, J. Yin, Z. Sun, S. Li, and T. Zhou, "Characterization of gas-liquid two-phase flow by correlation dimension of vortex-induced pressure fluctuation," *IEEE Access*, vol. 5, pp. 10307–10314, 2017.

[6] H. Y. Zhang, X. Tian, X. Deng, and Y. Cao, "Batch process fault detection and identification based on discriminant global preserving kernel slow feature analysis," *ISA Trans.*, vol. 79, pp. 108–126, May 2018.

[7] J. Wang and Q. P. He, "Multivariate statistical process monitoring based on statistics pattern analysis," *Ind. Eng. Chem. Res.*, vol. 49, no. 17, pp. 7858–7869, 2010.

[8] H. Wang, J. Chen, and G. Dong, "Feature extraction of rolling bearing's early weak fault based on EEMD and tunable Q-factor wavelet transform," *Mech. Syst. Signal Process.*, vol. 48, nos. 1–2, pp. 103–119, Oct. 2014.

[9] Z. Wu and N. E. Huang, "Ensemble empirical mode decomposition: A noise-assisted data analysis method," *Adv. Adapt. Data Anal.*, vol. 1, no. 1, pp. 1–41, 2008.

[10] M. E. Torres et al., "A complete ensemble empirical mode decomposition with adaptive noise," in *Proc. IEEE Int. Conf. Acoust.*, May 2011, vol. 125, no. 3, pp. 4144–4147.

[11] M. A. Colominas, G. Schlotthauer, and M. E. Torres, "Improved complete ensemble EMD: A suitable tool for biomedical signal processing," *Biomed. Signal Process. Control*, vol. 14, pp. 19–29, Nov. 2014.

[12] W. Li, M. Peng, and Q. Wang, "Fault detectability analysis in PCA method during condition monitoring of sensors in a nuclear power plant," *Ann. Nucl. Energy*, vol. 119, pp. 342–351, Sep. 2018.

[13] A. Phinyomark, H. Hu, P. Phukpattaranont, and C. Limsakul, "Application of linear discriminant analysis in dimensionality reduction for hand motion classification," *Meas. Sci. Rev.*, vol. 12, no. 3, pp. 82–89, May 2012.

[14] H. Gharahbagheri, S. Imtiaz, and F. Khan, "Combination of KPCA and causality analysis for root cause diagnosis of industrial process fault," *Can. J. Chem. Eng.*, vol. 95, no. 8, pp. 1497–1509, 2017.

[15] Y. Wang, P. W. Tse, Y. Qin, L. Deng, T. Huang, and B. Tang, "Kurtogram manifold learning and its application to rolling bearing weak signal detection," *Measurement*, vol. 127, pp. 533–545, Oct. 2018.

[16] X. He and P. Niyogi, "Locality preserving projections," in *Proc. Adv. Neural Inf. Process. Syst.*, 2005, vol. 45, no. 1, pp. 186–197.

[17] T. Zhang, J. Yang, D. Zhao, and X. Ge, "Linear local tangent space alignment and application to face recognition," *Neurocomputing*, vol. 70, nos. 7–9, pp. 1547–1553, 2007.

[18] N. E. Huang et al., "The empirical mode decomposition and the Hilbert spectrum for nonlinear and non-stationary time series analysis," *Proc. Roy. Soc. London A, Math., Phys. Eng. Sci.*, vol. 454, no. 1971, pp. 903–995, Mar. 1998.

[19] P. Flandrin, G. Rilling, and P. Goncalves, "Empirical mode decomposition as a filter bank," *IEEE Signal Process. Lett.*, vol. 11, no. 2, pp. 112–114, Feb. 2004.

[20] A. Humeau-Heurtier, G. Mahé, and P. Abraham, "Multi-dimensional complete ensemble empirical mode decomposition with adaptive noise applied to laser speckle contrast images," *IEEE Trans. Med. Imag.*, vol. 34, no. 10, pp. 2103–2117, Oct. 2015.

[21] X. Zhang, Y. Liang, and J. Zhou, "A novel bearing fault diagnosis model integrated permutation entropy, ensemble empirical mode decomposition and optimized SVM," *Measurement*, vol. 69, pp. 164–179, Jun. 2015.

[22] J. P. Amezquita-Sanchez, M. Valtierra-Rodriguez, and C. A. Perez-Ramirez, "Fractal dimension and fuzzy logic systems for broken rotor bar detection in induction motors at start-up and steady-state regimes," *Meas. Sci. Technol.*, vol. 28, no. 7, p. 057001, 2017.

[23] F. Li, B. Tang, and R. Yang, "Rotating machine fault diagnosis using dimension reduction with linear local tangent space alignment," *Measurement*, vol. 46, no. 8, pp. 2525–2539, 2013.

[24] R. Bos, S. D. Waele, and P. M. T. Broersen, "Autoregressive spectral estimation by application of the Burg algorithm to irregularly sampled data," *IEEE Trans. Instrum. Meas.*, vol. 51, no. 6, pp. 1289–1294, Dec. 2002.

[25] Z. Su, B. Tang, Z. Liua, and Y. Qin, "Multi-fault diagnosis for rotating machinery based on orthogonal supervised linear local tangent space alignment and least square support vector machine," *Neurocomputing*, vol. 157, pp. 208–222, Jun. 2015.

[26] Y. He, C. Y. Du, C. B. Li, A. G. Wu, and Y. Xin, "Sensor fault diagnosis of superconducting fault current limiter with saturated iron core based on SVM," *IEEE Trans. Appl. Supercond.*, vol. 24, no. 5, Oct. 2014, Art. no. 5602805.

[27] T. W. Rauber, F. de A. Boldt, and F. M. Varejão, "Heterogeneous feature models and feature selection applied to bearing fault diagnosis," *IEEE Trans. Ind. Electron.*, vol. 62, no. 1, pp. 637–646, Jan. 2015.

[28] S.-W. Fei and X.-B. Zhang, "Fault diagnosis of power transformer based on support vector machine with genetic algorithm," *Expert Syst. Appl.*, vol. 36, no. 8, pp. 11352–11357, 2009.

Authors' photographs and biographies not available at the time of publication.

• • •